TABLE I. Grade of Programmed EN Dieting

Step	Staple food (form of rice)	Side dishes (approved foods and cuisines)	Nutritive value
0	Liquid	Juice (without grain, without oranges), electrolytic supplement solution	500–2000 ml
1	Liquid	Water gruel, starch gruel, clear soup, consomme, juice, miso soup	Calories 300–350 kcal Protein 5–7 g Fat 15–2 g Dietary fiber 15 g
2	Mush	Potato, vegetables, canned fruits, vegetable juices, noodles, tofu, whitefish	Calories 600–650 kcal Protein 20–25 g Fat 5–8 g Dietary fiber 1.5–8 g
3	Rice gruel	Eggs, breads, banana, apple	Calories 900–1000 kcal Protein 30–35 g Fat 10–13 g Dietary fiber 8–9 g
4	Boiled rice	Blue-skinned fish, oil (~3 g/day)	Calories 1200–1300 kcal Protein 40–45 g Fat 15–20 g Dietary fiber 9–10 g
5	Boiled rice	Chicken (low fat), yogurt, oil (~8 g/day)	Calories 1500–1600 kcal Protein 60–65 g Fat 30–35 g Dietary fiber 12–13 g

Note: A patient-oriented stepped-up dieting program was gradually applied over six steps that varied with regard to the solidity, intensity, and acceptability by the patient.

of the GI system. Moreover, it has recently been reported that enteral nutrition (EN) was more effective than parenteral nutrition for the nutritional support of patients with an injured intestine due to trauma or an invasive operation [4,5]. Taken together, these findings suggest that the current patient management procedure that includes the interruption of oral feeding to enforce "bowel rest" in SCT patients suffering from GVHD should be critically reevaluated. Furthermore, EN, if tolerable, may be a preferred route for maintaining digestive and absorptive function as intact as possible.

In those suffering from GI involvement of GVHD, such evaluation becomes more complex since diarrhea is very often multifactorial and includes secretory dysfunction, osmotic factors, and rapid passage. Hence, the establishment of a standard care procedure remains very difficult. To address these concerns, we conducted a controlled cohort study to evaluate the benefit of different nutritional support measures for patients suffering from acute gut GVHD after SCT. Our clinical hypothesis was that a programmed and controlled scheduled oral nutritional support with EN is beneficial for patients who have mild to moderately progressing acute symptoms of gut GVHD.

PATIENTS AND METHODS

Patients

Seventy patients who were treated at the National Cancer Center Hospital from January 2001 to December 2003 and who developed GI symptoms by GVHD were involved in this prospective study. Forty among those eligible patients met the following inclusion criteria: (i) pathologically diagnosed GVHD with biopsied specimens, (ii) presented symptoms within 100 days after SCT, and (iii) clinically diagnosed as stage I to III gut GVHD and grade II to III acute GVHD according to the clinical grading criteria [6,7]. Patients who had intestinal tract bleeding, intestinal obstruction, or severe pancreatitis were excluded from this analysis, since these pathophysiologies are considered contraindications for EN. Additionally, patients with pathologically diagnosed cytomegalovirus enterocolitis were also excluded, and thus a total of 35 patients were left for this study.

Methods

In the study periods, two different nutritional intervention procedures were applied; patients who developed gut GVHD before July 2002 ($n = 17$) were treated with NPO and total parenteral nutrition (TPN) (C group), while the remaining patients who developed gut GVHD after July 2002 ($n = 18$) were treated by programmed GVHD dieting intervention (EN group). The patients were consecutively registered to our database at National Cancer Center Hospital, and this prospective study was approved by the IRB. The programmed EN dieting consisted of six steps with regard to solidity, intensity, and acceptability for intestinal digestion, as shown in Table I. Each food and nutrient was made more solid and dense

in a step-up manner, after the confirmation of stable symptoms that lasted for a minimum of 3 days. Each step of programmed EN dieting was suitably stepped down when intolerance or exacerbation of gut GVHD symptoms developed. Patients were made NPO with the appearance of significant abdominal symptoms (nausea, vomiting, and abdominal pain). Patients in the EN group only received oral intake without enteral tube feeding. On the other hand, the patients in group C were adequately allowed to eat according to their symptoms with TPN.

We evaluated "time to complete dietary recovery," which was defined as the duration from the start of nutritional management (stopping oral intake or start of programmed EN dieting) to the restoration of a normal diet with the recovery of nutritional parameters. Nutritional parameters evaluated in this study included (1) clinical symptoms, including volume and frequency of diarrhea, and body weight and (2) laboratory data, including total serum protein and albumin. Body mass index (BMI) was calculated as BMI = {height (m)}2/body wt (kg).

Statistical Analysis

Our clinical hypothesis was that a programmed and controlled schedule of nutritional support with oral intake (EN dieting) could be effective in the support of patients suffering from acute gut GVHD with mild to moderately progressing symptoms. We evaluated "the time to complete dietary recovery," which was defined as the duration from the start of nutritional management (stopping oral intake or start of EN dieting) to the recovery to normal diet, various enteral symptoms, and nutritional parameters. The time to complete dietary recovery is shown with a time–event cumulative curve, and the log-rank test was used to compare groups C and EN. Nutritional parameters are given as the mean of each group by time course, and the data in groups C and EN were compared by an analysis of variance (ANOVA). A P value of less than 0.05 was considered significant.

RESULTS

Patients' Characteristics

The patients' clinical backgrounds are summarized in Table II, which shows that there are no essential differences between groups C and EN. Older patients tended to receive a reduced-intensity regimen more often than a conventional regimen.

Safety of Programmed EN Dieting

Throughout the study, no severe adverse events associated with nutritional intervention were observed, indicating that our procedure with gradual stepped-up or -down dieting was safe. No severe infectious episodes were observed in each group. EN dieting had to be terminated early in 2 of 18 cases due to prolonged GI symptoms and exacerbation of an underlying malignant disorder. There were 4 censored cases in group C, mainly due to recurrence of the basic malignant disorder.

TABLE II. Patients' Characteristics

	EN group (N = 18)	C group (N = 17)
Age median (range)	53 (22–64)	53 (23–69)
Sex male/female	12/6	14/3
Disease		
AML	6	8
MDS	3	2
ALL	4	2
CML	3	1
NHL	1	2
ATL	1	1
Solid tumors	0	1
Transplantation source		
BM	1	3
PBSC	17	14
Transplantation regimen		
Conventional	5	7
Reduced intensity	13	10
Donor HLA typing		
Full match	14	14
1 locus mismatch	4	0
2 loci mismatch	0	3
GVHD prophylaxis		
CSP alone	10	8
CSP + MTX	6	4
CSP + ATG	2	2
Others	0	3
Gut GVHD stage		
1	5	9
2	7	3
3	6	5
GVHD grade		
II	6	8
III	12	9
Onset day of gut GVHD (mean of day)	74	68

Note: Patients who underwent SCT and developed gut GVHD were enrolled in this study. Patients who developed gut GVHD before July 2002 (n = 17) were treated with no oral intake (C group), while the EN group (n = 18) was treated by programmed GVHD dieting. AMI, acute myelogeneous leukemia; MDS, myelodysplastic syndrome; ALL, acute lymphoblastic leukemia; CML, chronic myelogeneous leukemia; NHL, non-Hodgkin lymphoma; ATL, adult T-cell leukemia; BM, bonemarrow; PBSC, peripheral blood stem cell; CSP, cyclosporine; MTX, methotrexate; ATG, anti-thymocyte globulin.

Efficacy of Programmed EN Dieting

Although there was a wide variation in each patient in diarrhea volume and frequency of diarrhea, we adapted ANOVA to evaluate whether there is a statistically significant difference between the two groups

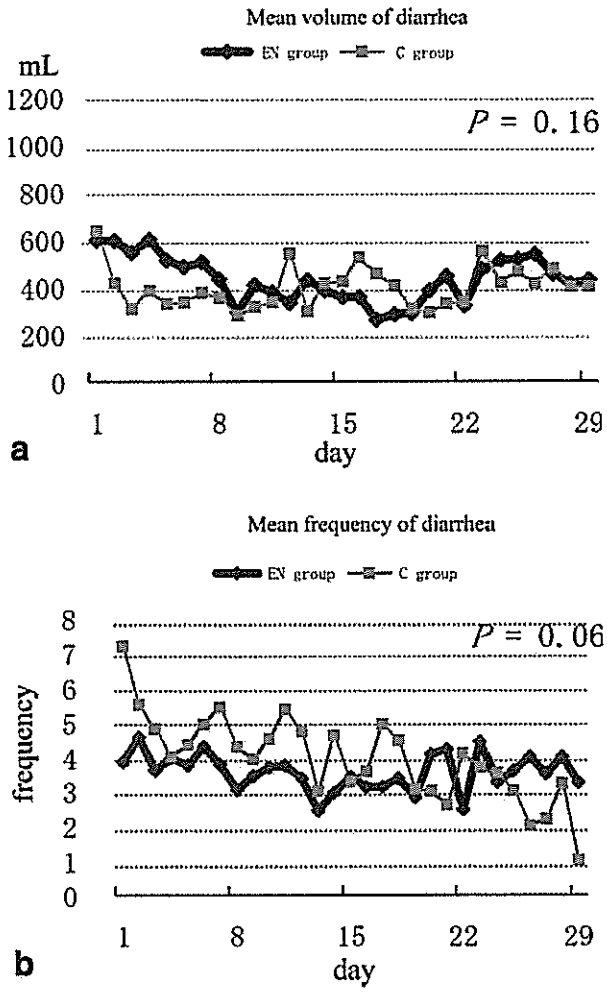

Fig. 1. Changes in mean volume and frequency of diarrhea. No difference was observed between the C and EN groups in the time-course of diarrhea as evaluated by volume ($P = 0.16$) (a) and frequency ($P = 0.06$) (b).

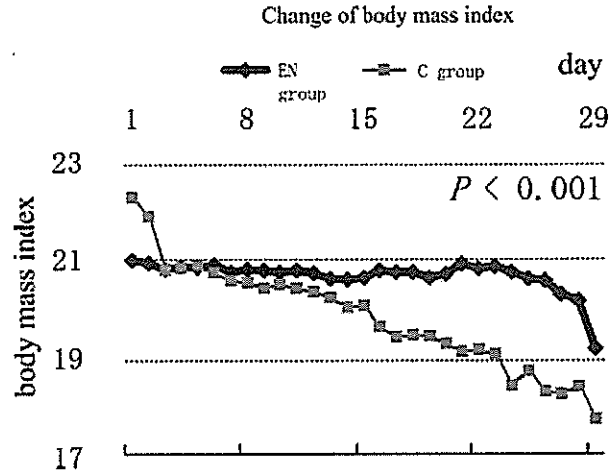

Fig. 2. Changes in BMI. The mean changes in BMI, with the first evaluation as a control, were compared between the two groups. A slower decrease in body weight tended to be observed in the EN group, while patients retained their BMI significantly better in the EN group than in the C group ($P < 0.001$). BMI was calculated as BMI = {height (m)}^{2}/body wt (kg).

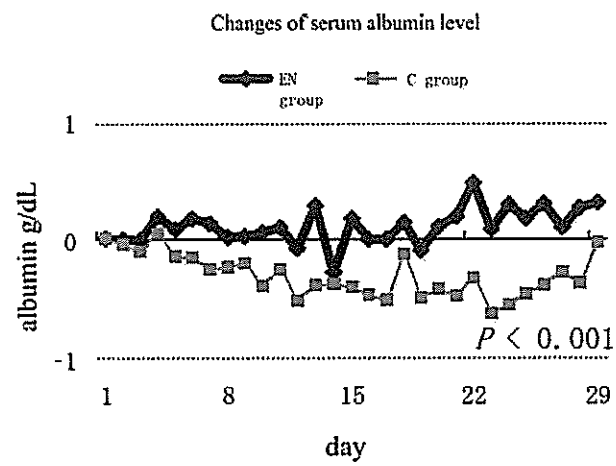

Fig. 3. Changes in albumin as nutritional parameter. One of the nutritional parameters, albumin (Alb), was evaluated between the C and EN groups. In the EN group, patients maintained significantly more stable levels of Alb ($P < 0.001$).

($P = 0.16$ and 0.06, respectively, Figure 1a and b). The mean body weight values in each group were compared by considering the absolute changes after adjusting by the value at the initial evaluation. In comparing the two groups, the decrease in body weight after the start of nutritional management was more obvious in group C than in group EN but this difference was not statistically significant ($P = 0.09$), since there was a wide interpatient variation. On the other hand, the change in BMI was significantly different between the two groups (Figure 2, $P < 0.001$).

Nutritional status was also estimated by laboratory parameters, including serum levels of total protein and albumin (Alb), which were determined as absolute changes by adjusting by the value at the first evaluation at the starting point of nutritional management, and a significantly slower decrease was noted in the EN group ($P < 0.001$) (Figure 3). These nutritional parameters remained higher in group EN than in group C. During the study period, no patient actually met with stopping rules mentioned above and consequently, the total number of days for NPO was not evaluated. The time to complete dietary recovery was compared between the two groups. While 38 days were required for the

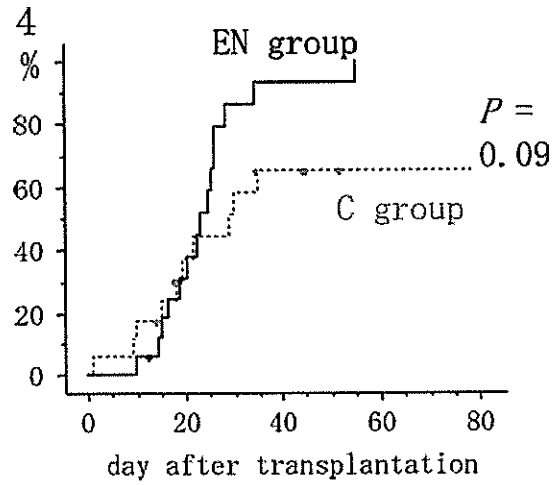

Fig. 4. Time to complete dietary recovery. The number of days required for return to a normal diet was 38 days in group C, while it was 31 days in group EN, with no statistically significant difference ($P = 0.09$).

recovery to a normal diet in group C, 31 days were required in group EN (Figure 4).

DISCUSSION

Since Weisdorf et al. reported that central venous parenteral nutritional support improved long-term survival in patients who underwent bone marrow transplantation (BMT) [8], intravenous TPN has been widely used in SCT. However, it has not yet been confirmed which procedure, enteral or parenteral nutrition, can provide more effective and safer nutritional support. In this study, we considered that the patients in the EN group may have preserved nutritional parameters better than the other group and ate sooner, although no differences were found in the time to complete dietary recovery. A clinical study group at Johns Hopkins University randomized BMT patients into two groups to receive different types of nutritional support, TPN or EN, and they did not observe any differences in nutritional parameters between the two groups [9]. In their study, patients who received TPN were allowed to eat anything they liked, while those with EN had few chances to receive TPN treatment. Moreover, those who had been receiving TPN were allowed to take oral intake and thus were not on strict NPO. Additionally, in our study, the two groups of patients were evaluated in different study periods, and there was a significant difference in the modality of the supportive measures. These points make a direct and strict comparison between the TPN and EN groups very difficult and unreliable. These biases, which are inherent to studies in this field, also existed in our study, which might explain why we failed to detect significant differences in clinical benefits.

We used to routinely advise patients to stop oral intake with the development of gut GVHD. Thereafter, they were encouraged to drink or eat gradually, since it has been suggested that inadequate nutritional support further deteriorates gut GVHD symptoms. To establish clearly defined subjective guidelines, we conducted this interventional cohort study. We found that both controlled and uncontrolled EN can be administered safely. Since the time to complete dietary recovery was almost comparable in the two groups, the results suggest that any EN program is acceptable and does not harm or degrade the QOL of patients suffering from GVHD. If this is confirmed, a restricted diet would not be necessary for those with moderately symptomatic gut GVHD. Nevertheless, the evaluation of nutritional parameters in this study suggested that controlled EN did a better job of maintaining body weight and serum nutritional status, compared to the results in the NPO group. The random administration of food intake may be inadequate compared to scheduled dieting, which attempts a gradual build-up of intestinal mucosa by the comprehensive supply of nutrients including glucose, protein, fat, fiber, etc. This may have a secondary advantage of keeping the mucosal barrier intact and preventing bacterial translocation through the GI tract.

Nevertheless, since the cause of diarrhea is multifactorial, it is inherently difficult to assess the effectiveness of and standardize nutritional intervention procedures. In the literature, four pathologies have been reported to be contraindications for EN since they cause undesirable bowel movement, i.e., presence of gastrointestinal bleeding, intestinal obstruction, severe pancreatitis, and intestinal perforation. The pathophysiology of diarrhea associated with gut GVHD includes osmotic and secretory diarrhea. Hypertonic EN is considered to further deteriorate symptoms of diarrhea. Hence, it is reasonable to suggest that dietary foods in EN adequately maintain an isotonic status as well as nutritional status to improve immunologic function. An intact GI system is vital for maintaining normal immune functions, and a novel concept of nutrition support, "immunonutrition," has been introduced, which focuses on the maintenance of the comprehensive biological protection system against external pathogens to maintain normal immune function [10]. Clinical benefits of immunonutrition, including improvement of nutritional parameters, decreased risk of infection, and shorter duration of hospitalization, have been reported in patients in the perioperation period and in those who required care in the ICU [11,12]. However, currently a precise evaluation

of the efficacy of each component of immunonutritional agents is difficult [13], and controversy still exists regarding the value of immunonutrition after SCT. This study did not evaluate this proposed immunonutrition, and to accomplish this in SCT practice, prospective monitoring of immune parameters would be required.

The serum level of albumin can be significantly affected by many variables including diarrhea associated with GVHD and, hence, would not be a very good marker for the evaluation of protein status in the HSCT population. However, in our experience, serum albumin decreased after SCT to suggest the possibility of the use in the estimation of patient's nutrition status at least for a short period of follow-up, when referring to the general description in the guideline by American Society for Parenteral and Enteral Nutrition, i.e., "low serum levels indicate which hospitalized patients are at increased risk of morbidity and mortality" [14].

In conclusion, the current study is hampered by preexisting biases including a small number of studied patients, a cohort analysis in different periods, and a lack of adequate measures for data evaluation. Nevertheless, it appears that patients supported by programmed EN experienced no exacerbation of gut GVHD symptoms, with a suggested benefit of enhanced maintenance of nutrition status. Further study is warranted to prospectively evaluate the value of various nutrients including arginine, o-3 fatty acid, and nucleic acid [13] and various clinical outcomes including the cost, complications, and QOL in an attempt to improve the nutritional and immune status of transplanted patients.

REFERENCES

1. Antin JH. Clinical practice. Long-term care after hematopoietic-cell transplantation in adults. N Engl J Med 2002;347:36–42.
2. Welsh FK, Farmery SM, MacLennan K, et al. Gut barrier function in malnourished patients. Gut 1998;42:396–401.
3. Weisdorf SS, Schwarzenborg SJ. Hematopoietic cell transplantation, 2nd ed. Nutritional support of hematopoietic stem cell recipients. Oxford: Blackwell; 1999. p 723.
4. Moore FA, Moore EE, Jones TN, et al. TEN versus TPN following major abdominal trauma—reduced septic morbidity. J Trauma 1989;29:916–922; discussion 922–923.
5. Archer SB, Burnett RJ, Fischer JE. Current uses and abuses of total parenteral nutrition. Adv Surg 1996;26:165–189.
6. Thomas ED, Storb R, Clift RA, et al. Bone-marrow transplantation (second of two parts). N Engl J Med 1975;292:895–902.
7. Przepiorka D, Weisdorf D, Martin P, et al. 1994 Consensus Conference on Acute GVHD Grading. Bone Marrow Transplant 1995;15:825–828.
8. Weisdorf SA, Lysne J, Wind D, et al. Positive effect of prophylactic total parenteral nutrition on long-term outcome of bone marrow transplantation. Transplantation 1987;43:833–838.
9. Szeluga DJ, Stuart RK, Brookmeyer R, et al. Nutritional support of bone marrow transplant recipients: a prospective, randomized clinical trial comparing total parenteral nutrition to an enteral feeding program. Cancer Res 1987;47:3309–3316.
10. Suchner U, Kuhn KS, Furst P. The scientific basis of immunonutrition. Proc Nutr Soc 2000;59:553–563.
11. Lipman TO. Grains or veins: is enteral nutrition really better than parenteral nutrition? A look at the evidence. J Parenter Enter Nutr 1998;22:167–168.
12. Heyland DK, Novak F, Drover JW, et al. Should immunonutrition become routine in critically ill patients? A systematic review of the evidence. J Am Med Assoc 2001;286:944–953.
13. Gianotti L, Braga M, Fortis C, et al. A prospective, randomized clinical trial on perioperative feeding with an arginine-, omega-3 fatty acid-, and RNA-enriched enteral diet: effect on host response and nutritional status. J Parenter Enter Nutr 1999;23:314–320.
14. Guidelines for the use of parenteral and enteral nutrition in adult and pediatric patients: A.S.P.E.N. Board of directors. J Parenter Enter Nutr 1993;17:5SA–6SA.

Tohoku J. Exp. Med., 2006, **210**, 125-135

Early Detection of Plasma Cytomegalovirus DNA by Real-Time PCR after Allogeneic Hematopoietic Stem Cell Transplantation

YASUSHI ONISHI,[1,3] SHIN-ICHIRO MORI,[1] AKIKO HIGUCHI,[2] SUNG-WON KIM,[1] TAKAHIRO FUKUDA,[1] YUJI HEIKE,[1] RYUJI TANOSAKI,[1] TOSHIO MINEMATSU,[4] YOICHI TAKAUE,[1] TAKESHI SASAKI[3] and KOH FURUTA[2]

[1]*Hematopoietic Stem Cell Transplantation Unit, and* [2]*Clinical Laboratory Division, National Cancer Center Hospital, Tokyo, Japan,*
[3]*Department of Rheumatology and Hematology, Tohoku University School of Medicine, Sendai, Japan, and*
[4]*Department of Microbiology, Miyazaki Medical College, Miyazaki, Japan*

ONISHI, Y., MORI, S., HIGUCHI, A., KIM, S., FUKUDA, T., HEIKE, Y., TANOSAKI, R., MINEMATSU, T., TAKAUE, Y., SASAKI, T. and FURUTA, K. *Early Detection of Plasma Cytomegalovirus DNA by Real-Time PCR after Allogeneic Hematopoietic Stem Cell Transplantation.* Tohoku J. Exp. Med., 2006, **210** (2), 125-135 —— Cytomegalovirus (CMV) infection is an important cause of morbidity and mortality after allogeneic hematopoietic stem cell transplantation. Therefore, preemptive ganciclovir therapy based on early detection of CMV reactivation is widely used to prevent CMV disease. Real-time polymerase chain reaction (PCR) has been widely used for monitoring CMV reactivation as well as the antigenemia assay that detects CMV structural phosphoprotein with a molecular weight of 65,000 (pp65). We developed a real-time PCR assay system for CMV based on a double-stranded DNA-specific dye, SYBR Green I, and quantified DNA, which was extracted automatically from plasma. This real-time PCR assay and the pp65 antigenemia assay were compared in parallel with 357 blood samples obtained from 64 patients who underwent allogeneic hematopoietic stem cell transplantation (allo-HSCT). Real-time PCR assay results correlated with those of the pp65 antigenemia assay ($p < 0.0001$). It is noteworthy that the detection of CMV DNA by PCR preceded the first positive antigenemia by 14 days. In this study, 10 of 64 patients developed CMV disease. The antigenemia assay detected CMV reactivation earlier than the development of CMV disease only in four of 10 patients. In contrast, our real-time PCR detected CMV-DNA before the development of CMV diseases in eight of 10 patients. The real-time PCR with SYBR Green I as a detection signal is simple and readily performed, and may be a useful system for early detection of CMV reactivation after allo-HSCT. ——— cytomegalovirus; real-time PCR; SYBR Green I; allogeneic hematopoietic stem cell transplantation; ganciclovir

Received July 11, 2006; revision accepted for publication August 21, 2006.
Correspondence: Yoichi Takaue, M.D., Hematopoietic Stem Cell Transplantation Unit, National Cancer Center Hospital, 5-1-1 Tsukiji, Chuo-ku, Tokyo 104-0045, Japan.
e-mail: ytakaue@ncc.go.jp

Cytomegalovirus (CMV) continues to be a major cause of morbidity, and this occasionally leads to the death of patients after allogeneic hematopoietic stem cell transplantation (allo-HSCT) (Boeckh et al. 2003). Although ganciclovir is an effective agent for CMV infection and disease, the administration of ganciclovir causes various adverse effects, including myelosuppression and nephrotoxicity. Therefore, it is important to discriminate high-risk patients from others to avoid over-treatment. Approaches that ganciclovir is used only in high-risk patients based on monitoring of CMV reactivation are called preemptive therapies. Preemptive therapies based on the antigenemia assay which detects CMV structural phosphoprotein with molecular weight of 65,000 (pp65) as a guide for starting ganciclovir have been widely used in clinical settings (Boeckh et al. 1996; Kanda et al. 2002a, b). However, this assay requires processing within 8 hrs of sampling, is time-consuming and suffers from a lack of standardization (Boeckh et al. 1994). Moreover, it lacks the sensitivity needed to predict the occurrence of CMV gastroenteritis (Boeckh et al. 1996; Mori et al. 2004), and can not be used when the leukocyte count is very low (Boeckh et al. 1997).

The direct detection of CMV DNA based on PCR has been investigated as an alternative measure for monitoring CMV infection, but qualitative PCR may not be able to discriminate between clinically significant and insignificant reactivation in immunocompromised individuals. On the other hand, studies using quantitative PCR have been shown to be useful for detecting patients at high risk of developing CMV disease (Gor et al. 1998). Real-time PCR, one modality of quantitative PCR, is a simple, reliable, cost-effective, and time-saving alternative strategy (Holland et al. 1991). Many institutes have developed real-time PCR assays for monitoring CMV, and have reported encouraging results (Gault et al. 2001; Cortez et al. 2003; Li et al. 2003; Nitsche et al. 2003; Ikewaki et al. 2005), where a dual-labeled fluorogenic hybridization probe or two single-labeled probes have been used to monitor PCR product formation.

Recently, a novel real-time PCR technique using a fluorescence dye, SYBR Green I, which upon binding to double-stranded DNA exhibits fluorescence enhancement, has been developed. This is the simplest real-time PCR technique based on the detection of PCR products by DNA-intercalating dye of SYBR Green I (Karsai et al. 2002). The use of SYBR Green I dye provides great flexibility and reduced cost because no target-specific probes are required. We have designed a new real-time CMV PCR assay that incorporates this system (Higuchi et al. 2002). Since cell separation from whole blood and DNA extraction could strongly affect the assay's reproducibility, we used plasma instead of peripheral blood mononuclear cells (PBMC), and a MagNA Pure automated DNA extraction instrument to automatically extract DNA from plasma. These changes made our real-time CMV PCR system much simpler than previously reported. In this study, we compared the laboratory and clinical feasibilities of this newly developed real-time CMV PCR using SYBR Green I with the existing pp65 antigenemia assay, which has been widely used as a guide for starting ganciclovir after allo-HSCT.

Materials and Methods

Patients and samples

We tested 357 blood samples obtained from 64 consecutive patients who underwent allo-HSCT and achieved sustained engraftment in our center between April 2003 and January 2004. The blood samples for the CMV antigenemia and real-time PCR were collected once a week from day 5 - 9 after transplantation until leaving our hospital. The study was approved by the National Cancer Center Institutional Review Board. All patients gave their written informed consent. The characteristics of these patients are shown in Table 1.

Stem cell transplantation procedure

Conditioning regimens and graft-versus-host disease (GVHD) prophylaxis are shown in Table 1. Fludarabine- or cladribine-based reduced intensity regimens were used in 47 patients and conventional myeloablative regimens were used in 16. Another patient did not receive any conditioning treatment before transplantation because he had severe bone marrow suppression and bacterial

TABLE 1. Characteristics of 64 patients.

Sex (Male/Female)	38/26
Median age in years (range)	47 (17 - 68)
Underlying disease	
Acute nonlymphoblastic leukemia	16
Acute lymphoblastic leukemia	8
Myelodysplastic syndrome	7
Malignant lymphoma	26
Agnogenic myeloid metaplasia	1
Plasma cell neoplasm	2
Solid tumor	4
Conditioning regimen	
Cyclophosphamide/TBI 12 Gy	6
Busulfan/Cyclophosphamide	10
Fludarabine/Busulfan	15
Fludarabine/Busulfan/TBI 4 Gy	18
Fludarabine/Busulfan/ATG	1
Fludarabine/Melphalan/TBI 4 Gy	1
Cladribine/Busulfan	8
Cladribine/Busulfan/TBI 4 Gy	2
Cladribine/Busulfan/ATG	2
Other	1
Type of donor	
HLA-identical sibling	32
HLA-mismatched family	4
Unrelated donor	28
Type of graft	
Bone Marrow	18
Blood stem cells	34
Cord blood stem cells	12
GVHD prophylaxis	
Cyclosporin A	23
Cyclosporin A/Methotrexate	38
Tacrolimus	3
CMV serostatus (recipient/donor)	
+/+	40
+/-	9
+/ ND	10
-/+	3
-/-	2

*TBI, total body irradiation; ATG, anti-thymocyte globulin; GVHD, graft-versus-host disease; CMV, cytomegalovirus; ND, no data.

infection after reinduction chemotherapy with idarubicin and cytosine arabinoside. Cyclosporine A alone, Cyclosporine A with methotrexate or tacrolimus alone, orally or intravenously was given to prevent GVHD. Ciprofloxacin, fluconazole, and sulfamethoxazole/trimethoprim were given as prophylaxis for bacterial, fungal, and pneumocystis carinii infections. All patients were given acyclovir 750 mg/day orally from day -7 to the discontinuation of GVHD prophylaxis.

CMV antigenemia assay

CMV antigenemia assay was performed by the method described previously (van der Bij et al. 1988; Gondo et al. 1994). In brief, 150,000 peripheral blood leukocytes were cytocentrifuged on a slide and fixed with acetone within 6 hours after specimen collection. The cells were incubated with monoclonal antibody horseradish peroxidase-C7 (Teijin, Tokyo) raised against the pp65 antigen of CMV, and stained by the direct immunoperoxydase method. Under light microscopy, CMV antigen-positive cells were enumerated. The degree of antigenemia was expressed as the number of positively stained cells per 50,000 leukocytes.

Amplification and detection of viral DNA

DNA was extracted from 200 μl of blood plasma with a MagNA Pure instrument (Roche Molecular Biochemicals, Mannheim, Germany). A MagNA Pure LC DNA Isolation Kit I was used according to the manufacturer's instructions. In the initial 42 samples, DNA was extracted manually using a QIAmp Blood mini-kit (Qiagen, Valencia, CA, USA).

We selected and designed the sequences of primers in the UL75 region of CMV. The forward and reverse primers of UL75 were 5′-CCT TGC GTG TCG TCG TAT TCT AGC-3′, and 5′-GCC TCA TCA TCA CCC AAA CGG ACA G-3′, respectively. PCR amplification was performed in a total volume of 20 μl in the presence of 2 μl of DNA sample, 4.4 μl of PCR master mix (Takara Ex Taq R-PCR Version, Takara, Shiga), 10 pmol of each of the primers, 2 mmol of $MgCl_2$, 2 μl (1 : 15,000 dilution) of Syber Green I (SYBR Green I Nucleic Acid Gel Stains, Takara), and distilled water.

PCR was performed with a LightCycler instrument using the SYBR Green I system (Roche Diagnostics, Tokyo) under the following conditions: 95°C for 30 sec and 35 cycles at 95°C for 0 sec (i.e., an instrument setting of zero seconds), 57°C for 5 sec, and 72°C for 10 sec. Crossing points were determined by the operator dependent fit points method. Melting curve analysis was performed on all of the positive results. The melting temperature range used to determine that a specimen yielding a crossing point was a true positive was 86.5 to 87.5°C.

Positive control and negative control

Positive PCR product DNA from a clinical sample was confirmed based on its positivity in electrophoresis and selected as the PCR standard. A direct sequence analysis was performed on this PCR product, which was confirmed to show a 100% match with GenBank data (NC_001347, similar as AD169 strain). The DNA from this sample was then subjected to molecular cloning by being inserted into the pCR4-TOPO vector (TOPO cloning kit, Invitrogen, Carlsbad, CA, USA). This plasmid was used as the CMV standard in this study. CMV was quantified using serially diluted CMV standards within the range of 1.41×10 to 1.41×10^8 copies per μl, and the numbers of CMV copies were calculated. The specificity of the CMV PCR was assessed by testing murine CMV (Smith strain) and herpes simplex viruses (HSV) (HSV-1; KOS strain and HSV-2; Savage strain) as negative controls. The CMV PCR assay with 35 cycles was negative for these samples.

Preemptive therapy for prevention of CMV disease

The decision to start preemptive therapy was based on the detection of 10 or more positive cells per 50,000 cells by the antigenemia assay, or by the clinical diagnosis of CMV disease with apparent or infection-related symptoms. In this study, PCR results were not used in the decision-making process regarding preemptive therapy. Intravenous ganciclovir was started at 5 mg/kg/day three times per week, and was continued until the positive cell count had decreased to less than 10 per 50,000 cells. If the number of positive cells increased or CMV-related symptoms worsened, the dose of ganciclovir was increased.

Statistical analysis and definition of CMV infection

Correlations between the number of CMV DNA and CMV antigen-positive cells were analyzed by calculating Spearman ranked correlation coefficient. Differences between two groups were assessed by the Mann-Whitney's U-test. ROC (Receiver Operating Characteristic) analysis was performed using ROCKIT 0.9B (Dorfman et al. 1992). The diagnostic power of UL75-PCR was assessed by calculating of the Area

under the ROC Curve (AUC). We accessed several cut-off values for positive cells, 1, 5, 10, or 50 per 50,000 examined cells, in the antigenemia assay to reflect "positive for CMV infection" on the ROC analysis. *P* values less than 0.05 were considered statistically significant.

Results

Clinical sample amplification

Threshold cycle values of the serially diluted standard were plotted (Fig. 1A), and showed good linearity (Fig. 1B). The amplification results of

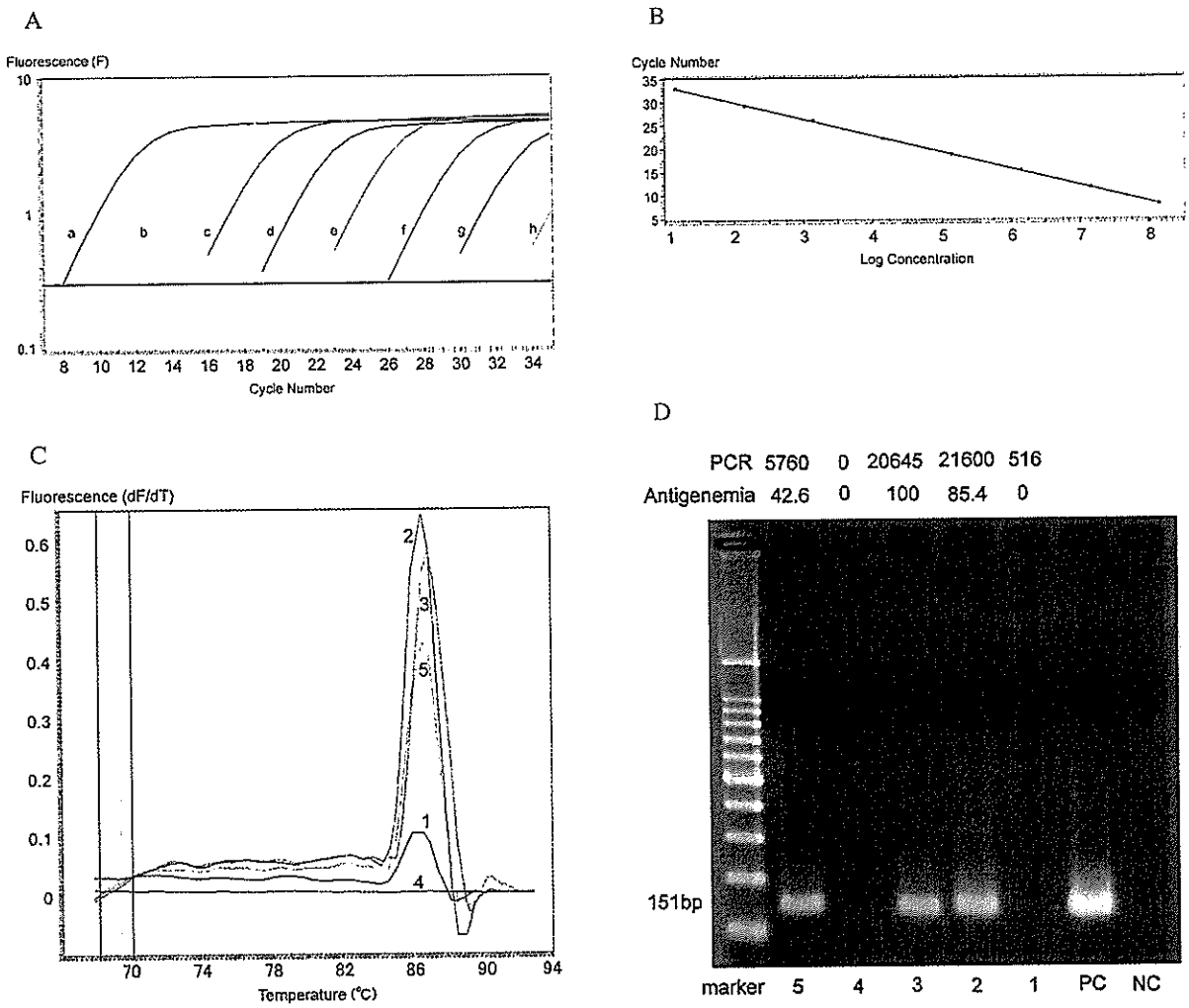

Fig. 1. Real-time PCR for CMV.

(A) Amplification plots obtained with the control plasmid for CMV. Serial 10-fold dilutions with 1.41×10^8 (a) to 1.41×10 (h) copies per reaction were amplified for 35 cycles. The horizontal line represents threshold of fluorescence signal. (B) Crossing points (cycle number) plotted against the log of copy number to obtain a calibration curve. The assay was linear from 1.41×10 to 1.41×10^8 copies per μl. (C) Melting curves for PCR products of five randomly selected clinical samples are shown. No extra peak was observed. (D) Amplification of PCR was confirmed by 2% agarose gel electrophoresis, which showed tight single bands, except in lanes 1 and 4. The numbers in upper line above the gel indicate the copy numbers per ml in cases 1, 2, 3, 4 and 5. The numbers in lower line above the gel indicate the corresponding results of the antigenemia test per 50,000 examined cells. Panels (C) and (D) share the same case numbers. The expected size of the PCR product is 151 bp. PC, positive control; NC, negative control.

five randomly selected clinical samples are shown as representative data. To confirm the purity of amplification, melting curves for PCR products after amplification were examined and the presence of an extra peak was neglected (Fig. 1C). Furthermore, amplification was confirmed by 2% agarose gel electrophoresis. Three of five samples showed a tight single 151 base-pair band in each lane, except lanes 1 and 4 (Fig. 1D), indicating that only one product was amplified. As a reference, the calculated copy numbers and the results of the antigenemia test for these samples are shown in Fig. 1D.

Comparison of the pp65 antigenemia assay with CMV real-time PCR

A total of 357 weekly samples were obtained from 64 patients and analyzed by both real-time PCR and antigenemia assays. As a result, a total of 158 samples obtained from 40 patients were positive for antigenemia assay, 220 samples from 55 patients were positive for real-time PCR which were confirmed by electrophoresis and melting curve analysis, 113 samples were negative for both assays, and 134 were positive for both assays (Kappa = 0.53). Eighty-six samples were positive by real-time PCR and negative by the antigenemia assay, while 24 samples were negative by real-time PCR and positive by the antigenemia assay (Table 2). The median number of pp65-positive cells in these 24 samples was 2 (range, 1.4 – 10.3) per 50,000 leukocytes.

There was a correlation between the CMV DNA copy number and the pp65-positive cell count (R = 0.738, $p < 0.0001$ by the Spearman test) (Fig. 2). Samples from patients were classified into four groups according to the results of the antigenemia assay (Fig. 3). Group 1 ($n = 199$) was negative by the antigenemia assay, group 2 ($n = 75$) was positive at 1 to 9 cells, group 3 ($n = 42$) was positive at 10 to 49 cells, and group 4 ($n = 41$) was positive at > 50 cells. The median CMV DNA load was 0 copies/ml (range, 0 to 39,345) in group 1, 344 (2.5 $\log_{10}$) copies/ml (0 to 172, 750) in group 2, 4,910 (3.7 $\log_{10}$) copies/ml (0 to 141,650) in group 3, and 22,200 (4.3 $\log_{10}$) copies/ml (2,285 to 464,750) in group 4. The CMV DNA load was significantly different in each group, as shown in Fig. 3 ($p < 0.0001$ by the Kuruskal-Wallis test). The specimens negative by real-time PCR or the antigenemia test are not depicted on the graphs in Fig. 2 and 3.

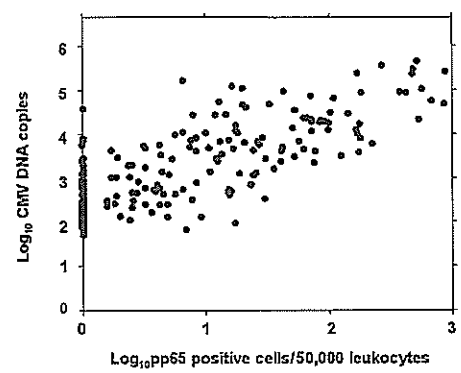

Fig. 2. Correlation between CMV DNA copy number in plasma and CMV pp65-positive cells. The CMV copy number was plotted on a logarithmic graph against the number of pp65-positive cells. The correlation between the two tests was examined (R = 0.738, $p < 0.0001$ by the Spearman test). The specimens negative by real-time PCR or the antigenemia test are not depicted. Minimum value by real-time PCR was 52 copies/ml.

TABLE 2. Results of real-time CMV PCR and CMV pp65 antigenemia of blood plasma for 357 samples.

CMV pp65 antigenemia	CMV PCR in blood plasma		Total
	Positive	Negative	
Positive	134	24	158
Negative	86	113	199
Total	220	137	357

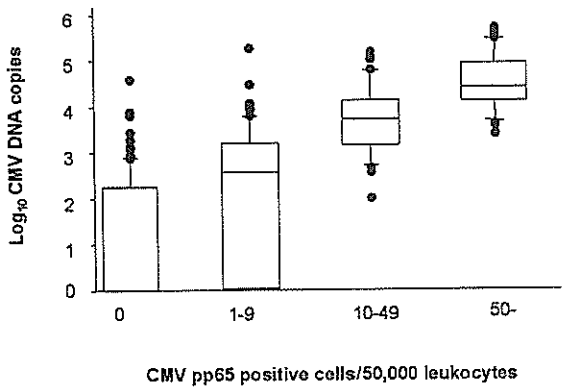

Fig. 3. CMV DNA loads in plasma based on the number of CMV pp65-positive cells per 50,000 leukocytes. Samples were classified into four groups: group 1 (n = 199), negative by the antigenemia assay; group 2 (n = 75), 1 to 9 positive cells; group 3 (n = 42), 10 to 49; and group 4 (n = 41), 50 and more. The median CMV DNA levels in samples were 0 copies/ml (range, 0 to 39,345), 344 (2.5 $\log_{10}$) copies/ml (range, 0 to 172,750), 4910 (3.7 $\log_{10}$) copies/ml (0 to 141,650), and 22,200 (4.3 $\log_{10}$) copies/ml (2,285 to 464,750), respectively. The CMV DNA load was significantly different among the four groups ($p < 0.0001$ by the Kuruskal-Wallis test). The box-and-whisker plots show 10th, 25th, 50th, 75th, 90th percentile values. The specimens negative by real-time PCR are not depicted. Outliers are indicated by dots.

Longitudinal analysis of the first detection of CMV DNA and CMV antigenemia cells

The CMV PCR and CMV antigenemia assays became positive simultaneously in 13 of 64 patients. The first positive PCR test preceded the first positive antigenemia by 14 days (7 to 35) in 20 patients, while the first positive antigenemia preceded the first positive PCR by 7 days in 4 patients. CMV PCR alone was positive in 18 patients, and CMV antigenemia alone was positive in 3 patients. Neither CMV PCR nor CMV antigenemia was positive in 6 patients. The median number of days for the first development of positive antigenemia and PCR results after transplantation was 34 days (12 to 141) and 20 days (12 to 97), respectively. Therefore, CMV PCR was positive significantly earlier than the CMV antigenemia assay ($p < 0.0001$ by the Mann Whitney's U-test). The WBC count at the first development of positive PCR was significantly lower, with a median of 2,700/μl (range, 100 to 27,400) than at the first positive antigenemia, with a median of 4,700/μl (700 to 40,900, $p = 0.027$ by Mann Whitney's U-test). In 23 of 64 patients, preemptive ganciclovir therapy was started upon the detection of 10 or more positive cells per 50,000 cells by the antigenemia assay at a median of day 39 (range, 18 to 122) after transplantation. Despite the preemptive therapy, five of 23 patients developed CMV disease at a median of day 50 (38 to 123) after transplantation. In five of 64 patients, ganciclovir was started based on the clinical diagnosis of CMV disease with apparent or infection-related symptoms at a median of day 38 (34 to 42).

Incidence of CMV disease

Ten of the 64 patients developed CMV disease. The time pattern of PCR and antigenemia detection relative to the onset of CMV disease in the 10 patients is shown in Fig. 4. Eight patients had CMV colitis, one had CMV retinitis (patient no. 8 in Fig. 4), and one had CMV pneumonia (patient no. 3). In these 10 cases, cord blood transplants were performed in three cases, transplants from an HLA-mismatched unrelated donor were performed in two, transplant from an HLA-matched unrelated was performed in one, transplant from an HLA-mismatched sibling was performed in one, and transplants from an HLA-identical sibling were performed in three. The median number of days to the onset of CMV disease was 42 days after transplant (33 to 123 days). CMV reactivation was detected 3 days or more before the development of CMV disease in 8 of 10 patients by real-time PCR. However, CMV antigenemia detected CMV reactivation earlier than the development of CMV disease only in 4 of 10 patients (Fig. 4). Five patients with CMV disease were successfully treated with ganciclovir and are currently alive, but the other five patients with CMV disease died from causes other than CMV disease. None of the patients in this series died of causes directly related to CMV disease.

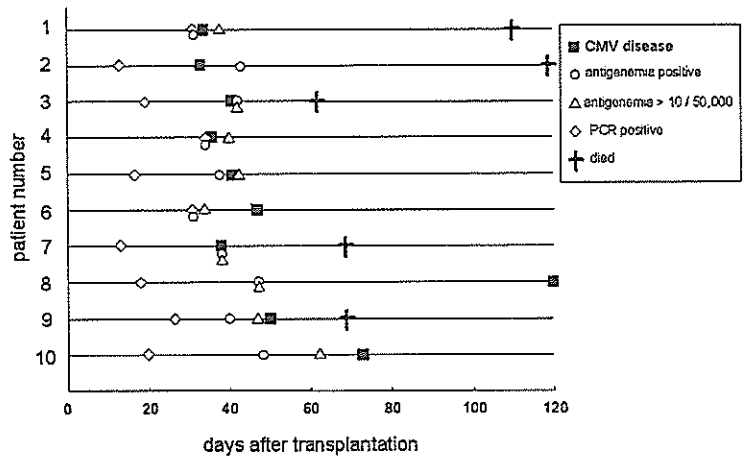

Fig. 4. Clinical course of individual patients with CMV disease. Solid squares, onset of CMV disease; open circles, first positive antigenemia; open triangles, first detection of > 10 positive cells per 50,000 cells by the antigenemia assay; open diamonds, first positive real-time PCR; cross, date of death.

The five deaths were caused by acute GVHD in one, disease progression in one, fungal infection in one, and bacterial infection in two. The peak CMV DNA load was significantly higher in patients with CMV disease, with a median of 82,250 copies/ml (range, 1,468 to 464,750) than in those without CMV disease, with a median of 628 copies/ml (0 to 374,150, $p = 0.005$, by Wilcoxon test).

Receiver Operating Characteristic (ROC) curve analysis

The ROC curves for UL75 PCR are shown in Fig. 5, in which four cut-off points for positive antigenemia, 1, 5, 10, or 50 positive cells per 50,000, were used. The LightCycler assay was clearly better than the discrimination limit. The Area Under the ROC Curve (AUC) values were 0.8426, 0.9240, 0.9483, and 0.9564, respectively, when 1, 5, 10, and 50 positive cells was used as a cut-off point for positive antigenemia. The 95% confidence intervals were as follows: 0.7917 – 0.8846, 0.8831 – 0.9529, 0.9205 – 0.9677, and 0.9311 – 0.9736, respectively. When the cut-off point was based on 10 pp65-positive cells per 50,000 cells, there was a better correlation between the CMV antigenemia assay and CMV PCR than when the cut-off point was based on 1

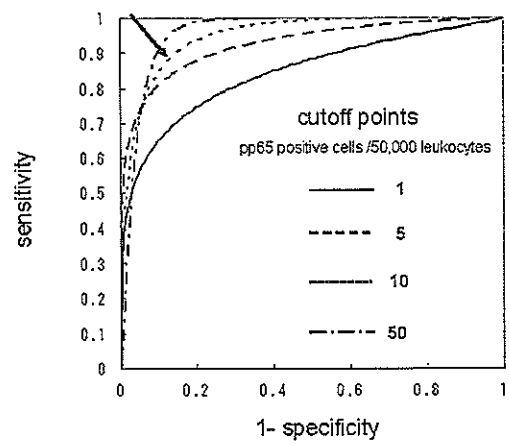

Fig. 5. ROC curves for UL75 PCR, with four cut-off points for the positivity for antigenemia: 1, 5, 10, or 50 cells per 50,000. The assay was far better than the discrimination limit. The AUC (Area Under the ROC Curve) values are 0.8426, 0.9240, 0.9483, and 0.9564, respectively. The 95% confidence intervals are as follows: 0.7917 – 0.8846, 0.8831 – 0.9529, 0.9205 – 0.9677, and 0.9311 – 0.9736, respectively. A tentative cut-off point at copy number 1,600 (arrow) gave a sensitivity of 87.2% and a specificity of 87.9% on the ROC curve in which 10 pp65-positive cells was used as the threshold for positive antigenemia.

pp65-positive cell. The cut-off points based on 5, 10, and 50 pp65-positive cells did not significantly differ from each other by the ROC analysis. A tentative cut-off point at copy number 1,600, as indicated by the arrow in Fig. 5, gave a sensitivity of 87.2% and specificity of 87.9% on the ROC curve, where 10 pp65-positive cells was used as the threshold for positive antigenemia.

Discussion

In our study, the CMV DNA copy number determined by real-time CMV PCR using SYBR Green I correlated with the number of pp65-positive cells, in agreement with the results of other studies using a TaqMan-based assay (Gault et al. 2001; Sanchez et al. 2001; Leruez-Ville et al. 2003; Li et al. 2003; Ikewaki et al. 2005). ROC analysis showed that this real-time CMV PCR exhibited adequate sensitivity and specificity, using the pp65 antigenemia assay as a reference standard. Corresponding to a pp65 antigenemia value of 10 positive cells per 50,000 leukocytes, which is used as the cutoff point for initiating preemptive therapy at our institute, a CMV DNA load of 1,600 copies/ml will be proposed as a cutoff point. However, we might have to start preemptive ganciclovir therapy at a cut off value of less than 1,600 copies/ml for high-risk patients. Our real-time PCR detected CMV-DNA earlier than the antigenemia assay detected CMV reactivation in the patients with CMV disease. Our real-time PCR makes it possible to adjust timing to start preemptive therapy more accurately according to the risk for CMV disease. The risks for CMV infection and/or disease have been increasing as new strategies have been introduced in allo-HSCT, including reduced-intensity stem cell transplantation, which enables older and/or heavily pretreated patients to undergo allo-HSCT, and HLA-mismatched transplantation with T-cell depletion or anti-T-cell agents (Kanda et al. 2001a; Nakai et al. 2002). Furthermore, Tomonari et al. (2003) suggested that the recovery of CMV-specific immunity after cord blood transplantation is delayed compared to that after BMT. Hence, in highly immunocompromised recipients, it may be advisable to set a lower cutoff point for the CMV DNA load to prevent CMV disease at the earliest stage. In this study, 47 patients underwent reduced-intensity stem cell transplantations (RIST) and 16 patients underwent conventional myeloablative stem cell transplantations (CST). The incidence of positive CMV antigenemia in the RIST group (33 of 47 patients, 70%) was higher than in the CST group (6 of 16 patients, 38%, $p = 0.019$). However, there was no significant difference in the incidence of positive PCR (85% and 88%) and CMV disease (17% and 13%) between the RIST group and the CST group. A higher incidence of CMV disease (10 of 64 patients, 16%) was observed and this might be attributed to our preemptive protocol consisting of a higher cutoff point and a lower initial dose of ganciclovir. It has been reported that preemptive therapy based on CMV antigenemia let to the more frequent development of CMV diseases other than pneumonitits, including gastrointestinal (GI) diseases, retinitis, and hepatitis (Boeckh et al. 1996; Kanda et al. 2001b). Mori et al. (2004) reported that among 19 and 14 patients who developed CMV-GI disease, only 4 (21%) and 7 patients (50%), respectively, became positive for antigenemia and plasma real-time PCR before the onset of CMV-GI disease. On the other hand, our plasma real-time PCR could detect CMV-DNA before the development of devastating CMV diseases in eight of 10 patients. The immediate initiation of antiviral therapy at low CMV DNA levels may become critical for highly immunocompromised recipients.

The detection of PCR products by the DNA-intercalating dye SYBR Green I system is simpler, cheaper, and probably more sensitive, since many fluorescent labels, rather than a single molecule, are incorporated into the amplified fragment (Karsai et al. 2002). However, this technique is not sequence-specific, and consequently nonspecifically amplified PCR products and primer dimers will also be detected. Nevertheless, we performed a melting curve analysis and electrophoresis to confirm that specific PCR products were formed, and these demonstrated specific and reproducible results.

We chose plasma as an assay material since

it still can be used during neutropenia (Boeckh et al. 1997). Plasma does not require labor-intensive processing such as isolation, counting, and adjustment of the number of peripheral blood leukocytes (PBL) before final analysis. It does not necessarily require normalization by a housekeeping gene, which is needed in real-time PCR using whole blood or PBL (Gault et al. 2001; Li et al. 2003). Despite these advantages of plasma as an assay material, it was long considered to be a poor source for PCR-driven assays because of its low sensitivity. Since the presence of CMV is strongly associated with cell components, it is considered that samples that incorporate whole blood or PBL provide a more sensitive detection of virus than plasma (Boeckh et al. 1997). However, recent improvements in plasma-based PCR assay have provided high sensitivity and clinical usefulness (Boeckh et al. 2004; Kalpoe et al. 2004; Schvoerer et al. 2005). Leruez-Ville et al. (2003) reported that a smaller PCR target (74bp) could provide better quantitative results because CMV DNA of plasma might be highly fragmented. In their study, the sensitivity of the PCR test was equivalent for plasma and whole blood. Although we did not compare the sensitivities with different components of blood, we demonstrated that our plasma real-time PCR was more sensitive than CMV antigenemia, perhaps due to the use of SYBR green I, i.e., the PCR target used in this study was 151 bp, which is not small enough to explain the improved sensitivity.

DNA extraction could strongly affect the assay's reproducibility (Gault et al. 2001). Mengelle et al. (2003) demonstrated that automated extraction and quantification of DNA from whole blood, instead of separated and counted PBL, provided acceptable results. They reported that 3.4 $\log_{10}$ genome copies in 200 μl of whole blood was equivalent to a threshold value of 50 pp65-positive cells per 200,000 cells. We applied the automated extraction of DNA in plasma and demonstrated that the plasma sample had an equivalent sensitivity for preemptive therapy for CMV. Hong et al. (2004) also reported that the combination of automated plasma DNA preparation and real-time PCR detection allowed for a sensitive assay of CMV viral load after bone marrow transplantation. It is evident that the standardization of plasma separation and storage methods should improve the reproducibility of plasma CMV DNA assays, which may further support the value of automated DNA extraction.

Our real-time PCR system for the measurement of CMV DNA in plasma using automated extraction and SYBR Green I dye appears to be a practical and simple system for obtaining reliable data and early detection of CMV reactivation, particularly for the purpose of prospectively guiding preemptive therapy for CMV disease after allo-HSCT.

References

Boeckh, M., Woogerd, P.M., Stevens-Ayers, T., Ray, C.G. & Bowden, R.A. (1994) Factors influencing detection of quantitative cytomegalovirus antigenemia. *J. Clin. Microbiol.*, **32**, 832-834.

Boeckh, M., Gooley, T.A., Myerson, D., Cunningham, T., Schoch, G. & Bowden, R.A. (1996) Cytomegalovirus pp65 antigenemia-guided early treatment with ganciclovir versus ganciclovir at engraftment after allogeneic marrow transplantation: a randomized double-blind study. *Blood*, **88**, 4063-4071.

Boeckh, M., Gallez-Hawkins, G.M., Myerson, D., Zaia, J.A. & Bowden, R.A. (1997) Plasma polymerase chain reaction for cytomegalovirus DNA after allogeneic marrow transplantation: comparison with polymerase chain reaction using peripheral blood leukocytes, pp65 antigenemia, and viral culture. *Transplantation*, **64**, 108-113.

Boeckh, M., Nichols, W.G., Papanicolaou, G., Rubin, R., Wingard, J.R. & Zaia, J. (2003) Cytomegalovirus in hematopoietic stem cell transplant recipients: Current status, known challenges, and future strategies. *Biol. Blood Marrow Transplant.*, **9**, 543-558.

Boeckh, M., Huang, M., Ferrenberg, J., Stevens-Ayers, T., Stensland, L., Nichols, W.G. & Corey, L. (2004) Optimization of quantitative detection of cytomegalovirus DNA in plasma by real-time PCR. *J. Clin. Microbiol.*, **42**, 1142-1148.

Cortez, K.J., Fischer, S.H., Fahle, G.A., Calhoun, L.B., Childs, R.W., Barrett, A.J. & Bennett, J.E. (2003) Clinical trial of quantitative real-time polymerase chain reaction for detection of cytomegalovirus in peripheral blood of allogeneic hematopoietic stem-cell transplant recipients. *J. Infect. Dis.*, **188**, 967-972.

Dorfman, D.D., Berbaum, K.S. & Metz, C.E. (1992) Receiver operating characteristic rating analysis. Generalization to the population of readers and patients with the jackknife method. *Invest. Radiol.*, **27**, 723-731.

Gault, E., Michel, Y., Dehee, A., Belabani, C., Nicolas, J.C. & Garbarg-Chenon, A. (2001) Quantification of human cytomegalovirus DNA by real-time PCR. *J. Clin. Microbiol.*, **39**, 772-775.

Gondo, H., Minematsu, T., Harada, M., Akashi, K., Hayashi, S., Taniguchi, S., Yamasaki, K., Shibuya, T., Takamatsu, Y. &

Teshima, T. (1994) Cytomegalovirus (CMV) antigenaemia for rapid diagnosis and monitoring of CMV-associated disease after bone marrow transplantation. *Br. J. Haematol.*, **86**, 130-137.

Gor, D., Sabin, C., Prentice, H.G., Vyas, N., Man, S., Griffiths, P.D. & Emery, V.C. (1998) Longitudinal fluctuations in cytomegalovirus load in bone marrow transplant patients: relationship between peak virus load, donor/recipient serostatus, acute GVHD and CMV disease. *Bone Marrow Transplant.*, **21**, 597-605.

Higuchi, A., Kitamura, Y., Kami, M. & Furuta, K. (2002) Development of a real-time quantitative PCR assay for the detection of CMV on the LightCycler platform. Presented at the The 9th Annual Meeting of the Japanese society for Gene Diagnosis and Therapy, Kyoto.

Holland, P.M., Abramson, R.D., Watson, R. & Gelfand, D.H. (1991) Detection of specific polymerase chain reaction product by utilizing the 5′----3′ exonuclease activity of Thermus aquaticus DNA polymerase. *Proc. Natl. Acad. Sci. USA*, **88**, 7276-7280.

Hong, K.M., Najjar, H., Hawley, M. & Press, R.D. (2004) Quantitative real-time PCR with automated sample preparation for diagnosis and monitoring of cytomegalovirus infection in bone marrow transplant patients. *Clin. Chem.*, **50**, 846-856.

Ikewaki, J., Ohtsuka, E., Satou, T., Kawano, R., Ogata, M., Kikuchi, H. & Nasu, M. (2005) Real-time PCR assays based on distinct genomic regions for cytomegalovirus reactivation following hematopoietic stem cell transplantation. *Bone Marrow Transplant.*, **35**, 403-410.

Kalpoe, J.S., Kroes, A.C., de Jong, M.D., Schinkel, J., de Brouwer, C.S., Beersma, M.F. & Claas, E.C. (2004) Validation of clinical application of cytomegalovirus plasma DNA load measurement and definition of treatment criteria by analysis of correlation to antigen detection. *J. Clin. Microbiol.*, **42**, 1498-1504.

Kanda, Y., Mineishi, S., Nakai, K., Saito, T., Tanosaki, R. & Takaue, Y. (2001a) Frequent detection of rising cytomegalovirus antigenemia after allogeneic stem cell transplantation following a regimen containing antithymocyte globulin. *Blood*, **97**, 3676-3677.

Kanda, Y., Mineishi, S., Saito, T., Seo, S., Saito, A., Suenaga, K., Ohnishi, M., Niiya, H., Nakai, K., Takeuchi, T., Kawahigashi, N., Shoji, N., Ogasawara, T., Tanosaki, R., Kobayashi, Y., Tobinai, K., Kami, M., Mori, S., Suzuki, R., Kunitoh, H. & Takaue, Y. (2001b) Pre-emptive therapy against cytomegalovirus (CMV) disease guided by CMV antigenemia assay after allogeneic hematopoietic stem cell transplantation: a single-center experience in Japan. *Bone Marrow Transplant.*, **27**, 437-444.

Kanda, Y., Mineishi, S., Saito, T., Saito, A., Ohnishi, M., Niiya, H., Chizuka, A., Nakai, K., Takeuchi, T., Matsubara, H., Makimoto, A., Tanosaki, R., Kunitoh, H., Tobinai, K. & Takaue, Y. (2002) Response-oriented preemptive therapy against cytomegalovirus disease with low-dose ganciclovir: a prospective evaluation. *Transplantation*, **73**, 568-572.

Karsai, A., Muller, S., Platz, S. & Hauser, M.T. (2002) Evaluation of a homemade SYBR green I reaction mixture for real-time PCR quantification of gene expression. *Biotechniques*, **32**, 790-792, 794-796.

Leruez-Ville, M., Ouachee, M., Delarue, R., Sauget, A.S., Blanche, S., Buzyn, A. & Rouzioux, C. (2003) Monitoring cytomegalovirus infection in adult and pediatric bone marrow transplant recipients by a real-time PCR assay performed with blood plasma. *J. Clin. Microbiol.*, **41**, 2040-2046.

Li, H., Dummer, J.S., Estes, W.R., Meng, S., Wright, P.F. & Tang, Y.W. (2003) Measurement of human cytomegalovirus loads by quantitative real-time PCR for monitoring clinical intervention in transplant recipients. *J. Clin. Microbiol.*, **41**, 187-191.

Mengelle, C., Sandres-Saune, K., Pasquier, C., Rostaing, L., Mansuy, J.M., Marty, M., Da Silva, I., Attal, M., Massip, P. & Izopet, J. (2003) Automated extraction and quantification of human cytomegalovirus DNA in whole blood by real-time PCR assay. *J. Clin. Microbiol.*, **41**, 3840-3845.

Mori, T., Mori, S., Kanda, Y., Yakushiji, K., Mineishi, S., Takaue, Y., Gondo, H., Harada, M., Sakamaki, H., Yajima, T., Iwao, Y., Hibi, T. & Okamoto, S. (2004) Clinical significance of cytomegalovirus (CMV) antigenemia in the prediction and diagnosis of CMV gastrointestinal disease after allogeneic hematopoietic stem cell transplantation. *Bone Marrow Transplant.*, **33**, 431-434.

Nakai, K., Kanda, Y., Mineishi, S., Saito, T., Ohnishi, M., Niiya, H., Chizuka, A., Takeuchi, T., Matsubara, H., Kami, M., Makimoto, A., Tanosaki, R., Kunitoh, H., Tobinai, K. & Takaue, Y. (2002) Suspected delayed immune recovery against cytomegalovirus after reduced-intensity stem cell transplantation using anti-thymocyte globulin. *Bone Marrow Transplant.*, **29**, 237-241.

Nitsche, A., Oswald, O., Steuer, N., Schetelig, J., Radonic, A., Thulke, S. & Siegert, W. (2003) Quantitative real-time PCR compared with pp65 antigen detection for cytomegalovirus (CMV) in 1122 blood specimens from 77 patients after allogeneic stem cell transplantation: which test better predicts CMV disease development? *Clin. Chem.*, **49**, 1683-1685.

Sanchez, J.L., Kruger, R.M., Paranjothi, S., Trulock, E.P., Lynch, J.P., Hicks, C., Shannon, W.D. & Storch, G.A. (2001) Relationship of cytomegalovirus viral load in blood to pneumonitis in lung transplant recipients. *Transplantation*, **72**, 733-735.

Schvoerer, E., Henriot, S., Zachary, P., Freitag, R., Fuchs, A., Fritsch, S., Risch, S., Meyer, N., Caillard, S., Lioure, B. & Stoll-Keller, F. (2005) Monitoring low cytomegalovirus viremia in transplanted patients by a real-time PCR on plasma. *J. Med. Virol.*, **76**, 76-81.

Tomonari, A., Iseki, T., Ooi, J., Takahashi, S., Shindo, M., Ishii, K., Nagamura, F., Uchimaru, K., Tani, K., Tojo, A. & Asano, S. (2003) Cytomegalovirus infection following unrelated cord blood transplantation for adult patients: a single institute experience in Japan. *Br. J. Haematol.*, **121**, 304-311.

van der Bij, W., Torensma, R., van Son, W.J., Anema, J., Schirm, J., Tegzess, A.M. & The, T.H. (1988) Rapid immunodiagnosis of active cytomegalovirus infection by monoclonal antibody staining of blood leucocytes. *J. Med. Virol.*, **25**, 179-188.

Diabetologia (2006) 49:2948–2958
DOI 10.1007/s00125-006-0432-z

ARTICLE

Streptozotocin-induced partial beta cell depletion in nude mice without hyperglycaemia induces pancreatic morphogenesis in transplanted embryonic stem cells

F. Takeshita · M. Kodama · H. Yamamoto · Y. Ikarashi · S. Ueda · T. Teratani · Y. Yamamoto · T. Tamatani · S. Kanegasaki · T. Ochiya · G. Quinn

Received: 30 May 2006 / Accepted: 27 July 2006 / Published online: 18 October 2006

Abstract

Aims/hypothesis It appears that the adult pancreas has limited regenerative ability following beta cell destruction by streptozotocin (STZ). However, it is not clear if this limitation is due to an inability to respond to, rather than an absence of, regenerative stimuli. In this study we aimed to uncouple the regenerative signal from the regenerative response by using an exogenous stem cell source to detect regenerative stimuli produced by the STZ-injured pancreas at physiological blood glucose levels.

Method Adult nude mice received 150 mg/kg STZ and 1×10^6 J1 mouse embryonic stem (ES) cells by i.p. injection. Permanent beta cell depletion of 50% was estimated from the ratio of beta:alpha cells in pancreata from STZ-treated mice compared with control animals after 24 days.

Results Transplanted ES cells homed to the STZ-injured pancreas and formed tumours. Immunocytochemical analysis of pancreas-associated ES tumours revealed foci containing insulin/PDX-1 double-positive and glucagon-positive/PDX-1-negative cell clusters associated with PDX-1-positive columnar lumenal epithelium and extensive α-amylase-positive pancreatic acini comprising approximately 0.1% of ES tumour volume.

Conclusions/interpretation These data indicate that (1) the adult pancreas produces a milieu of regenerative stimuli following beta cell destruction, and (2) this is not dependent on hyperglycaemic conditions; (3) these regenerative stimuli appear to recapitulate the signalling pathways of embryonic development, since both exocrine and endocrine lineages are produced from PDX-1-positive precursor epithelium. This model will be useful for characterising the regenerative mechanisms in the adult pancreas.

Keywords α-amylase · Embryonic stem cells · Glucagon · Insulin · Morphogenesis · PDX-1 · Regeneration · Streptozotocin · Transplantation

Abbreviations

DAPI	4′,6-diamidino-2-phenylindole
E	embryonic day
ES	embryonic stem (cells)
ESM	Electronic supplementary material
IVIS	in vivo imaging system
PDX-1	pancreatic and duodenal homeobox protein-1
STZ	streptozotocin

Introduction

Current mainstream treatments for type 1 (insulin-dependent) diabetes are frequently dogged by risks of hypoglycaemic episodes, increased body weight and numerous lifestyle restrictions [1]. On the other hand, type 2 (non-

Electronic supplementary material Supplementary material is available in the online version of this article at http://dx.doi.org/10.1007/s00125-006-0432-z and is accessible to authorised users.

F. Takeshita · M. Kodama · H. Yamamoto · S. Ueda · T. Teratani · Y. Yamamoto · T. Ochiya · G. Quinn (✉)
Section for Studies on Metastasis,
National Cancer Center Research Institute,
1-1 Tsukiji, 5-chome, Chuo-ku,
Tokyo 104-0045, Japan
e-mail: garyquinn99@hotmail.com

T. Tamatani · S. Kanegasaki · G. Quinn
Effector Cell Institute, Research Center for Advanced Science and Technology (RCAST), University of Tokyo,
Tokyo, Japan

Y. Ikarashi
Pharmacology Division,
National Cancer Center Research Institute,
Tokyo, Japan

insulin-dependent) diabetes is spreading at an epidemic pace in the developing world. Hence, there is a pressing need for superior treatments, which will benefit from deciphering the mechanisms of islet beta cell regeneration. The adult pancreas has the ability to regenerate following injury by a variety of means, although this regenerative capacity appears to be limited [2–5].

Streptozotocin (STZ) is a glucose-conjugated nitrosourea taken up via the pancreas-specific GLUT2 transporter. A single high dose of STZ can induce acute hyperglycaemia by rapid necrosis of pancreatic beta cells within 24 h [3], while multiple low doses of STZ can produce a gradual onset of hyperglycaemia by T cell-mediated autoimmune destruction of beta cells, a model sharing characteristics with type 1 diabetes [6]. Early studies in the hyperglycaemic rodent indicated that following a high dose of STZ, some but not significant numbers of beta cells were recovered [7]. A lower dose of STZ, producing less severe hyperglycaemia, resulted in permanent beta cell damage with negligible replacement of beta cells from the duct [8, 9]. However, it is not clear from these studies whether the lack of beta cell recovery in STZ-treated animals with normal blood glucose levels resulted from an absence of regenerating factors or from an inability of potential endogenous beta cell progenitors to respond to nascent regenerating stimuli.

We reported that following transplantation, undifferentiated mouse embryonic stem (ES) cells migrated to the liver and formed tumours in animals with hepatic injury [10]. These ES cell tumours contained differentiated hepatocytes induced by regenerating factors from the injured liver. The aim of the present study was to investigate the lack of beta cell recovery by introducing an exogenous multi-potent cell source to the nude mouse following a single STZ dose that induced partial beta cell destruction with neither the induction of hyperglycaemia nor the knock-on effect of T cell-mediated further beta cell damage.

We investigate whether moderate STZ-induced pancreatic injury can stimulate induction of pancreas morphogenesis in transplanted ES cells as well as self-regeneration. This approach could be important for unravelling the adult pancreas regeneration process and for identifying potential soluble factors for in vitro differentiation of insulin-producing beta cells for the treatment of diabetes.

Materials and methods

Animals and STZ treatment

Animal experiments in the present study were performed in compliance with the guidelines of the Institute for Laboratory Animal Research at the National Cancer Center Research Institute (Tokyo, Japan). In addition, the Principles of Laboratory Animal Care (NIH publication no. 85-23, revised 1985; available from http://grants1.nih.gov/grants/olaw/references/phspol.htm, last accessed in July 2006) were followed. Female BALB/c nude mice (CLEA, Tokyo, Japan) aged 7 weeks were used as recipients for ES cell transplantation. Mice received a single 300-μl i.p. dose of STZ (Sigma Aldrich, St Louis, MO, USA) within 20 min of dissolution in freshly prepared 20 mmol/l cold citrate buffer (pH 4.5) at a dose ranging from 100 to 200 mg/kg body weight. Control mice received 300 μl citrate buffer alone. Duplicate glucose measurements were performed on whole venous blood collected from the tail vein of non-fasting animals at 48 h after STZ treatment and twice weekly thereafter, using the Freestyle Flash Blood Monitoring System (Nipro, Tokyo, Japan) according to the manufacturer's instructions. For investigation of the effect of STZ concentration on ES cell differentiation, 12 mice were used. Mice received ES cells 24 h after STZ injection by i.p. administration. All ES cells were injected on the same day and from the same cell preparation. The cell injection site was the lower abdomen, as far from the pancreas as possible. Physiological sample data at day 14 for these animals is shown in Table 1. For renal capsule transplantation experiments, 1×10^6 ES cells were transplanted 24 h following treatment of mice with 150 mg/kg STZ (n=2) or citrate buffer (n=2). Briefly, recipient mice were anaesthetised by exposure to 1–3% isoflurane, and a 1.5-cm cut through the skin and muscle of the left flank

Table 1 Physiological characteristics of animals transplanted i.p. with mouse embryonic stem cells

STZ treatment	Blood glucose (mmol/l)[a,b]	Weight (g)[a]	ES homing to pancreas?[a]
Citrate buffer #1	4.2	21.6	No
Citrate buffer #2	4.4	20.4	No
Citrate buffer #3	5.0	21.9	No
STZ 100 mg/kg #1	6.6	23.3	No
STZ 100 mg/kg #2	6.7	21.6	No
STZ 100 mg/kg #3	6.2	22.8	No
STZ 150 mg/kg #1	6.2	20.2	Yes
STZ 150 mg/kg #2	4.9	21.2	Yes
STZ 150 mg/kg #3	5.0	20.2	Yes
STZ 200 mg/kg #1	8.7	20.5	Yes
STZ 200 mg/kg #2	21.7	17.3	Yes
STZ 200 mg/kg #3	19.6	17.4	Yes

Relationship between STZ dose, blood glucose concentration (>11.1 mmol/l=hyperglycaemic) and effect on homing to the pancreas of transplanted mouse ES cells measured by in vivo imaging. Representative data is shown for mice at day 14. Blood glucose concentration remained similar to day 14 values for each animal until mice were killed on day 24. Average weight of mice at day 0=19±1 g.

[a] At day 14 post-treatment

[b] Average of two consecutive readings

dorsal to the spleen was made. The exposed wound was flushed with 1 ml PBS containing penicillin/streptomycin (Invitrogen, Carlsbad, CA, USA) and the kidney was pushed through the wound. A small cut was made laterally on the kidney membrane using a scalpel, and 10 μl PBS containing 1×10^6 ES cells was gently expelled towards the bottom of the kidney capsule using a 20-μl pipette tip. The kidney was replaced in the abdominal cavity, and the incision was closed with small wound clips. For i.v. transplantation, 1×10^6 ES cells in 100 μl PBS were injected via the tail vein 24 h after STZ treatment. For evaluation of induction of hormone-positive duct cells in the pancreas of STZ-treated mice, animals were treated with citrate buffer (group 1, n=3), 150 mg/kg STZ (group 2, n=6) or 200 mg/kg STZ (group 3, n=6), and killed 24, 48 and 72 h later (one in group 1, two in group 2, three in group 3 for each time point), and tissues were sectioned and stained for glucagon and insulin.

For estimation of permanent beta cell depletion in 150 mg/kg STZ- vs citrate buffer-injected mice, six animals were used. Mice were treated with 150 mg/kg STZ (n=3) or citrate buffer (n=3) and killed after 24 days, then pancreas sections were double-stained using immunofluorescence for glucagon and insulin as described below. All six mice had blood glucose concentrations <11.1 mmol/l throughout the 24-day period. Islets containing between 10 and 400 cells for each animal were photographed, and alpha and beta cells were counted using ImageJ software (version 1.31v) available from http://rsb.info.nih.gov/ij/download.html, last accessed in July 2006. For each islet, the ratio of beta:alpha cells was calculated and averaged for >30 islets per mouse (100 islets per group). For evaluation of the percentage of ES cell tumours occupied by pancreatic foci and PDX-1-positive foci ImageJ software was used to draw a closed perimeter around the foci and measure the sum of the areas occupied by these foci relative to the area of a closed perimeter drawn around the whole tissue section. This was repeated for several tissue sections from each mouse and averaged. For estimation of numbers of insulin-positive and PDX-1/insulin double-positive cells, individual cells were counted within the closed perimeter area of the ES cell tumour pancreatic foci only and their overall ES cell tumour proportion was then estimated.

Culture and in vivo transplantation of ES cells

The firefly luciferase-expressing ESJ1 cell line, a J1 cell clone of 129SV male origin, was established as described previously [11]. Twenty-four hours after STZ treatment, mice received 1×10^6 ES cells by single i.p. injection in 300 μl PBS prepared as described previously [11]. In vivo imaging analysis of transplanted ES cells was conducted in a cryogenically cooled IVIS system (Xenogen, Alameda, CA, USA). Mice were administered D-luciferin (150 mg/kg; Promega, Madison, WI, USA) by i.p. injection and anaesthetised by exposure to 1–3% isoflurane. Photons from animal whole bodies were counted 10 min later using the IVIS imaging system according to the manufacturer's instructions, and data were analysed using LIVINGIMAGE 2.50 software (Xenogen). The amount of light generated was directly related to the amount of luciferase-producing cells. The development of pancreatic ES cell tumours was monitored twice weekly.

Immunofluorescence and immunohistochemical analyses

Following killing of mice by cervical dislocation, pancreases and ES cell tumour tissues were preserved in 10% formalin solution, before being embedded in paraffin and sectioned. Sections were deparaffinised in xylene and rehydrated through a graded ethanol series. Antigen retrieval was performed by boiling sections for 5 min in 10 mmol/l citrate buffer followed by cooling for 30 min to room temperature. Blocking was carried out using Image-iT FX Signal Enhancer (Invitrogen) for 30 min at room temperature. Primary antibodies were applied overnight at 4°C. AlexaFluor secondary antibodies (1:1,000; Invitrogen) were applied for 30 min at room temperature. All antibodies were diluted in ChemMate Antibody Diluent (Dako, Kyoto, Japan). Immunofluorescence-stained sections were mounted with Vectashield mounting medium (Vector Laboratories, Burlingame, CA, USA) containing 4′, 6-diamidino-2-phenylindole (DAPI) to visualise nuclei. The following primary antibodies were used: anti-insulin (1:400, #MAB1417; R&D systems, Minneapolis, MN, USA), anti-glucagon (1:200, #sc-7779; Santa Cruz Biotechnology, Santa Cruz, CA, USA), anti-C-Peptide (1:400, #4023-01; Linco, St Charles, MO, USA), anti-HNF3β (1:100, #sc-9187; Santa Cruz) anti-PDX-1 (1:100, #07-696; Upstate, Charlottesville, VA, USA), anti-α-amylase (1:200, #A8273; Sigma) and anti-luciferase (1:100, #PM016; MBL, Woburn, MA, USA). Luciferase, HNF3β and α-amylase staining was performed using the Vectastain ABC kit (Vector Laboratories) according to the manufacturer's instructions, followed by haematoxylin or eosin counter-staining using standard methods.

Results

Beta cell neogenesis following STZ treatment

Doses of 150 mg/kg STZ or below consistently failed to induce overt hyperglycaemic blood glucose concentrations (>11.1 mmol/l) up to 4 weeks following treatment (Table 1; sample data is shown at day 14), while doses of 200 mg/kg

usually led to acute hyperglycaemia (blood glucose concentration >11.1 mmol/l) within 48 h, which was accompanied by sustained poor weight gain and polyuria thereafter. The lowest single STZ dose that can induce hyperglycaemia in mice is variable and dependent on genetic background for inbred strains. The BALB/c genetic background displays unusually high resistance to STZ-induced DNA damage, which is directly related to poly (ADP-ribose) polymerase (PARP) activation and NAD depletion [12]. This would explain why a STZ dose of 150 mg/kg, which is sufficient to induce rapid hyperglycaemia in some mouse strains, did not do so in this study. Nevertheless, since STZ degrades rapidly and mice treated with 150 mg/kg STZ did not develop elevated blood glucose levels in this study, an alternative method was necessary to establish that the STZ dose administered in this instance induced some degree of beta cell depletion. As STZ is a selective destroyer of beta cells, the alpha cell population should remain constant before and after treatment (unless there is an expansion of alpha cells during regeneration that has not previously been demonstrated). We therefore compared the average ratio of beta (insulin-positive): alpha (glucagon-positive) cells over a range of islet sizes from non-ES cell-transplanted control mice (n=3) and mice treated with 150 mg/kg STZ (n=3) 24 days after treatment. Using this approach we estimated that the average rate of permanent destruction of beta cells in euglycaemic mice treated with 150 mg/kg was 50% (Fig. 1). Between 24 and 48 h after 150 mg/kg STZ treatment, some ductal hormone-positive cells were detectable in the pancreas of treated mice, including occasional insulin/glucagon double-positive cells (data not shown). However, 24 days after treatment, hormone-positive duct cells were not detectable. In contrast, in hyperglycaemic mice treated with 200 mg/kg STZ, clusters of insulin-positive cells within the pancreatic ducts were common after 24 days (data not shown), as previously observed in the regenerating adult pancreas under hyperglycaemic conditions [13].

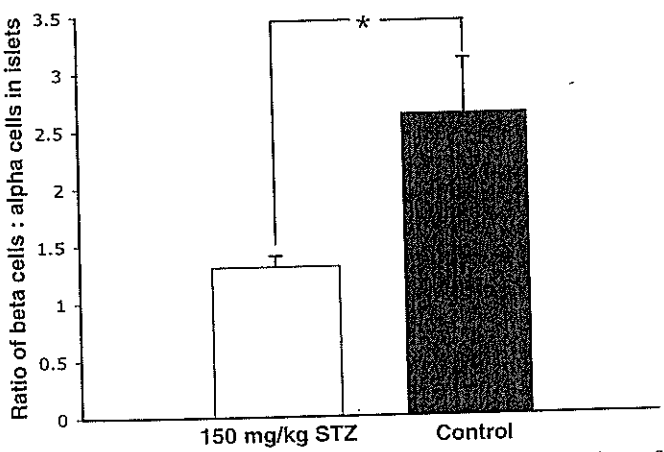

Fig. 1 Permanent beta cell depletion in the pancreatic islets of euglycaemic mice treated with STZ. Mice received 150 mg/kg STZ (*white bar*; n=3) or citrate buffer alone (*black bar*; n=3). The average ratio of beta (insulin-positive):alpha (glucagon-positive) cells in >100 islets per group at day 24 after STZ treatment revealed approximately 50% permanent beta cell depletion. Data are presented as means±SEM. *p<0.05, t test

Transplanted ES cells migrate to and proliferate in the STZ-injured pancreas

Pancreatic homing and proliferation of i.p. transplanted ES cells was clearly detectable by in vivo imaging in all animals that received doses of 150 mg/kg or 200 mg/kg STZ from day 14 after transplantation (Fig. 2). At lower STZ doses (100 mg/kg) and in citrate buffer-treated mice, homing to the pancreas was not detected in any animals up to day 24 when all mice were killed. Earlier attempts using i.v. transplantation of ES cells also gave rise to small peri-pancreatic tumours. However, these tumours developed more slowly than following i.p. transplantation (Electronic supplementary material [ESM] Fig. 1) and mice were prone to lethal pulmonary teratomas. All mice produced s.c. tumours at the site of injection, presumably due to some leaking of cells into the s.c. space during ES cell injection. In addition to s.c. tumours, small teratomas were occasionally observed at random sites (non-pancreas-associated) sites in the peritoneum of i.p. ES cell transplanted mice. Anatomical analysis of the pancreata of 150 mg/kg STZ-treated mice following killing at 24 days after ES cell injection revealed vascular networks interconnecting ES cell-derived tumour nodules with the vasculature of the host pancreas (Fig. 2), indicating that the movement of soluble factors between pancreas and ES cell tumour was facilitated during ES cell tumour growth and differentiation.

Transplanted ES cells differentiate into hormone-positive cell clusters in STZ-treated mice

ES cell-derived pancreatic tumours were analysed for expression of hormonal markers of pancreatic islet (alpha and beta) cells. Staining of serial ES cell tumour sections alternately for insulin and glucagon revealed foci with clusters of hormone-positive cells spatially associated with each other and arranged along the periphery of rosettes of large eosinophilic granular cells, which displayed histological similarity to pancreatic acini (Fig. 3c, inset). These acinar-like cells were hormone-negative. In addition, these ES cell tumour foci always contained lumenal columnar epithelium adjacent to the hormone-positive clusters. This epithelium showed weak hormone staining that was polarised towards the acinar-like and hormone-positive cell clusters and occasionally contained cells that stained strongly positive for glucagon or insulin (Fig. 3, arrowheads).